

Internal-inertial waves and cross-frontal circulation in the upper ocean

JOAQUÍN TINTORÉ and SERGIO ALONSO
Geophysical Fluid Dynamics Group, Dept. de Física
Universitat de les Illes Balears
07071 Palma, Spain

DONG-PING WANG
Marine Sciences Research Center
State University of New York
Stony Brook, NY 11794, USA

EMILIO GARCÍA
Dept. de Física
Universitat Autònoma de Barcelona
08193 Bellaterra, Spain

RESUMEN

Se estudia el proceso de ajuste entre dos masas de agua de propiedades diferentes y la circulación secundaria asociada, por medio de un modelo oceánico tridimensional de ecuaciones primitivas. En particular, se investiga la recirculación y el movimiento vertical cerca de un frente de densidad muy marcado, haciendo énfasis en los efectos de las ondas internas iniciales, con el fin de conocer su influencia en la circulación normal, en doble célula, observada en los frentes oceánicos de densidad. Se demuestra que esas ondas, generadas en el proceso de ajuste geostrófico, juegan un papel esencial en la intensificación de la circulación normal al frente y de la mezcla en los frentes de densidad. Los resultados teóricos obtenidos son aplicables al frente de densidad, permanente y muy intenso, observado en la zona oriental del Mar de Alborán, al sur de Cabo de Gata. Este frente es consecuencia de la convergencia de agua mediterránea y atlántica en la zona, ideal para verificar los resultados teóricos de este estudio.

ABSTRACT

Using a three dimensional primitive equation ocean model, we study the adjustment of two very distinct water masses and the associated circulation patterns. In particular, we investigate the recirculation and vertical motions near a very sharp density front with special emphasis on the effects of internal-inertial waves. The goal of this study is to clarify the importance and the effects of internal-inertial waves on the observed double cell cross-frontal circulation of oceanic density fronts. We show these waves, generated by geostrophic adjustment, play an essential role and enhance both cross frontal

circulation and mixing in oceanic density fronts. These theoretical results are applicable to the very intense and permanent density front present in the eastern Alboran Sea. This front develops south of Cape Gata as a result of the convergence of Mediterranean and Atlantic water and is therefore an ideal place to test the theoretical results of this study.

1. INTRODUCTION

Adjustment of a fluid under gravity occurs because of the natural tendency to reach an equilibrium. This problem was initially studied by Rossby (1937) who was concerned with how the pressure and velocity distributions in the atmosphere and the ocean evolve towards geostrophic equilibrium. Rossby, using the principle of conservation of potential vorticity, was able to find the final equilibrium state without knowing the exact details of the transient and highly nonlinear adjustment process.

The problem was reviewed by Gill (1982) and only a brief description will be given here. If a shallow, homogeneous, unbounded, non-rotating fluid, initially at rest and with a step-discontinuity in the surface elevation collapses at $t = 0$, a gravity-wave front is generated to either side. The final state has a level surface, the initial potential energy being completely converted to kinetic energy. In a rotating fluid, the fluid adjusts rapidly (in a time of the order of the rotation period) to an equilibrium state that is not a state of rest and that contains more potential energy than does the rest state. The final surface elevation is not level and the initial discontinuity has in the final state a characteristic width, the Rossby Radius of deformation. An important feature of this case is that the kinetic energy of the final state is only one-third of the potential energy released. The other two thirds, are commonly assumed to be radiated away by the gravity waves generated in the initial stage of the adjustment.

The linear adjustment of an initially motionless fluid with a vertical density interface has been studied among others by Csanady (1971, 1978), Gill (1976), Ou (1984), Van Heijst (1985) and Middleton (1987). All these studies were mainly concerned with the final equilibrium shape of the front. The transients have been less investigated: Kao *et al.* (1978) studied the circulation associated with a surface buoyant influx and found that at the head of the gravity current, the front is formed by intense sinking of fresh surface water. Wang (1984) examined the flow adjustment between two initially separated water masses and showed that intense mixing at the horizontal edge of the gravity current slowed down the front speed.

In the ocean, regions of intensified horizontal gradients (fronts) are often found between two different water bodies. Stationary ocean fronts represent the near equilibrium state reached between two different waters. A remarkable example of this type of fronts is the Almería-Orán front in the eastern Alboran Sea (Tintoré *et al.*, 1988). This front develops south of Cape Gata, is almost stationary and represents the near equilibrium state reached

between the lighter Atlantic water and the denser Mediterranean water. Associated with the density gradient, a well defined southeastward baroclinic jet with velocities around 100 cm/s has been also described.

Density fronts in the ocean are well known regions of increased biomass. These high levels of biomass have been usually related to the existence of a weak, almost permanent cross-frontal non linear circulation (James, 1978; Van Heijst, 1985; Simpson and James, 1986). Brink (1987) indicated that the existence of a cross-frontal circulation as the «double cell» circulation pattern proposed by Moores *et al.* (1976) has been a controversial subject over the years. Numerical studies (Kao *et al.*, 1978, James, 1978, 1984) have shown this type of cell patterns with surface convergence, upwelling and downwelling. However, the cross-frontal velocities obtained seem far too small to account (alone) for the observed higher biological activity.

The fore-mentioned numerical studies addressed the question of the near steady state circulation but did not consider the effects of the oscillatory motion also present in any adjustment problem. In fact, inertial oscillations appear associated with the long waves generated during the initial phase of the adjustment (Gill, 1976). Since these oscillations do not propagate away (zero group velocity) they are very difficult to damp, and their role in the adjustment of different fluids should be considered.

The aim of this study is to investigate the adjustment of two very distinct water masses and the associated circulation patterns. More specifically, the objective is to investigate the recirculation of the buoyant fluid and the vertical motions near a very sharp density front with special emphasis on the effects of gravity-inertial waves.

In a complex system such as the atmosphere or the ocean, we need to consider a simple experiment to try to understand the complicated dynamics associated with the adjustment to equilibrium. We have therefore considered an initial state in which two very different waters are initially separated by a vertical barrier. A main difference between this study and Wang (1984) is that while he investigated the mixing processes at the front during the initial stage of the adjustment, we are interested in the near steady-state cross-frontal ageostrophic circulation and on the effects of inertial-gravity waves. Also since this study was suggested by the cross-frontal circulation patterns observed in the Almería-Orán front (Tintoré *et al.*, 1988); the density difference is $1.5 \cdot 10^{-3}$ (g/cm³) and the light water does not reach the bottom of the basin. The recirculation in the upper layers (which is what we are really interested in) is therefore less influenced by the bottom induced circulation. To investigate the effect of bottom friction and its influence on damping the fluctuating part of the crossfrontal circulation we have studied the adjustment in two different basins. In the shallow case (100 m deep) the light water occupies the upper 80 m while in the deep one (500 m) the light water occupies the upper 300 m. This last case can be roughly assimilated with the adjustment taking place in the Eastern Alboran Sea.

2. THE MODEL

The numerical model used has been described by Wang (1982, 1984) and only a brief description is given here for completeness. It is a three dimensional primitive equation model but a two dimensional version of the model is used in this study for easier interpretation of the results. The model is then two-dimensional in a vertical plane, represents a cross-section perpendicular to the front and allows the development of the current component in the along-front direction. We have also assumed that the motion is hydrostatic and water is incompressible. Therefore, in cartesian coordinates, the governing equations are:

$$\frac{\partial u}{\partial t} + u \frac{\partial u}{\partial x} + w \frac{\partial u}{\partial z} - f v = -\frac{1}{\rho} \frac{\partial p}{\partial x} + \frac{\partial}{\partial x} \left(A_h \frac{\partial u}{\partial x} \right) + \frac{\partial}{\partial z} \left(A_v \frac{\partial u}{\partial z} \right) \quad (1)$$

$$\frac{\partial v}{\partial t} + u \frac{\partial v}{\partial x} + w \frac{\partial v}{\partial z} + f u = -\frac{1}{\rho} \frac{\partial p}{\partial y} + \frac{\partial}{\partial x} \left(A_h \frac{\partial v}{\partial x} \right) + \frac{\partial}{\partial z} \left(A_v \frac{\partial v}{\partial z} \right) \quad (2)$$

$$\frac{\partial p}{\partial z} + \rho g = 0 \quad (3)$$

$$\frac{\partial u}{\partial x} + \frac{\partial w}{\partial z} = 0 \quad (4)$$

$$\frac{\partial \rho}{\partial t} + u \frac{\partial \rho}{\partial x} + w \frac{\partial \rho}{\partial z} = \frac{\partial}{\partial x} \left(K_h \frac{\partial \rho}{\partial x} \right) + \frac{\partial}{\partial z} \left(K_v \frac{\partial \rho}{\partial z} \right) \quad (5)$$

where t is time, x , y and z the space coordinates, u and v the x - and y -components of the current velocity (offshore, alongshore), ρ is density, f the Coriolis parameter. Horizontal eddy coefficients are constant,

$$A_h = K_h = 10^5 \text{ cm}^2/\text{s} \quad (6)$$

Boundary conditions are:

At the free surface there is no surface stress:

$$A_v (\partial u / \partial z, \partial v / \partial z) = 0, \quad (7a)$$

$$K_v \partial \rho / \partial z = 0 \quad (7b)$$

At the ocean bottom there is bottom friction:

$$A_v (\partial u / \partial z, \partial v / \partial z) = -\lambda (u, v) \quad (8)$$

where λ is a linear drag coefficient (.1 cm/s).

At the coast, a free slip condition is assumed (the normal flow vanishes);

$$u = 0 \tag{9a}$$

$$A_h (\partial u / \partial x, \partial v / \partial x) = 0 \tag{9b}$$

$$K_h \partial \rho / \partial x = 0 \tag{9c}$$

At the open ocean, ambient conditions are specified as

$$\eta = 0 \tag{10a}$$

$$\rho = \rho^o(z) \tag{10b}$$

where η is the free surface elevation and ρ^o is the ambient density profile

The vertical eddy coefficients are the Munk-Anderson type (cm²/s):

$$A_v = A_v^o (1 + 10\text{Ri})^{-1/2}, \tag{11a}$$

$$K_v = K_v^o (1 + 3.33\text{Ri})^{-3/2}, \tag{11b}$$

where Ri is the local Richardson number,

$$\text{Ri} = - \frac{g}{\rho^o} \frac{\frac{\partial \rho}{\partial z}}{\left[\left(\frac{\partial u}{\partial z} \right)^2 + \left(\frac{\partial v}{\partial z} \right)^2 \right]^{1/2}} \tag{12}$$

and

$$A_v^o = K_v^o = 50 \text{ cm}^2/\text{s}$$

Initial conditions: we impose a very steep initial density distribution. The total length of our basin is 120 km and the two water masses are separated by a vertical wall, located at $x = x_o = 72$ km. The density difference is $\Delta\rho = \rho_2 - \rho_1 = 1.5 \sigma_t$ ($1.5 \cdot 10^{-3} \text{ g/cm}^3$).

$$\begin{aligned} \rho &= \rho_1, x < x_o \\ \rho &= \rho_2, x > x_o \end{aligned} \tag{14}$$

The numerical technique used is described in Wang (1982, 1984) and is standard for three dimensional multi-level models (Simmons, 1980). In essence, equations 1-5 are written in finite difference form in a staggered grid, figure 1. The scheme is leapfrog in time, centred in space (except for the

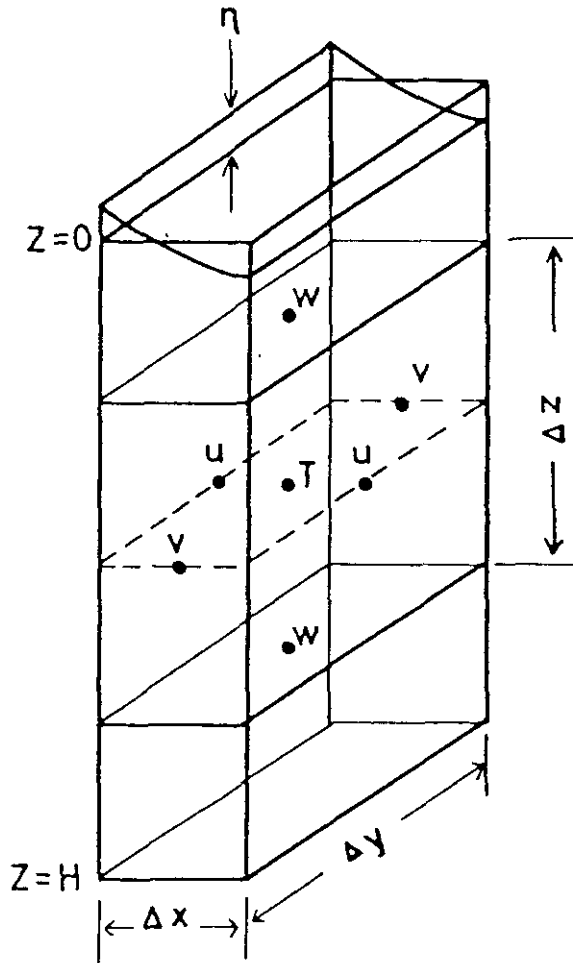


Figure 1.—Location of the basic variables on the finite difference C grid.

density equation where an upwind scheme is used) and uses a mode-split technique in the vertical direction and a semi-implicit scheme in the horizontal direction to achieve computational efficiency.

3. RESULTS

3.1. Non rotating case

This case, appropriate for adjustment processes taking place in short periods (e.g. river plumes, ...) is presented to emphasize the role of rotation in

any adjustment problem. The lock between the two water masses was released at $t = 0$ and we have followed the evolution of the adjustment until the front reached the open boundary.

3.1.1. *Basin 100 m deep*

The flow may be characterized by a velocity scale $U = (g'h)^{1/2}$, where h is the depth of the inflowing fluid and g' is the reduced gravity. In this case, $U = 107$ cm/s while the surface front propagates at a speed of 50 cm/s, figure 2. Therefore the front propagates at half the gravity wave speed, a result that was already found by Wang (1984) who also discussed it in terms of the energy transfer during the adjustment. It is important to observe that the light fluid is catching up the leading edge of the front, therefore inducing a strong convergence and downward motion. For example, at $t = 15$ h, the speed of the frontal bore was 85 cm/s ($\sigma_t = 27.25$) while the speed of the 28.0 isopycnal was significantly lower, 35 cm/s. The maximum vertical velocity obtained was 0.2 cm/s.

3.1.2. *Basin 500 m deep*

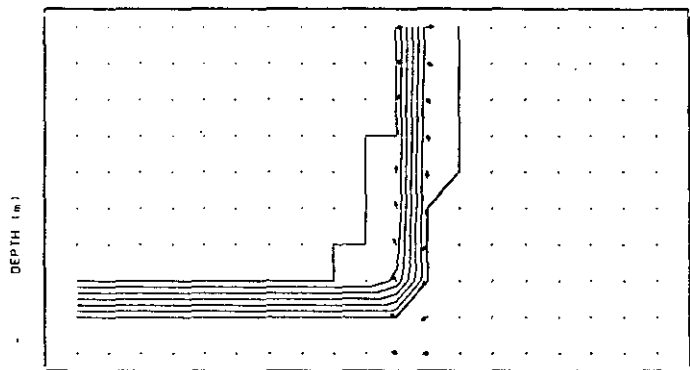
Since the depth of the basin is now 500 m and the depth of the buoyant fluid is 300 m, we expect the surface convergence to be stronger and as a result larger vertical velocities can be reached. The numerical simulation shows the propagation of the front is faster and after 10 h, the front has already reached the limits of our domain giving a speed of 160 cm/s, figure 3. For comparison, the characteristic velocity in this case is 207 cm/s. The vertical velocities induced are also extremely high, around 1 cm/s.

Comparison between these two cases shows the essential effect of the depth of the buoyant fluid (it is actually the fractional depth h/H which is an important parameter), a result which was already found in a tank experiment by Benjamin (1986).

3.2. **Rotating case**

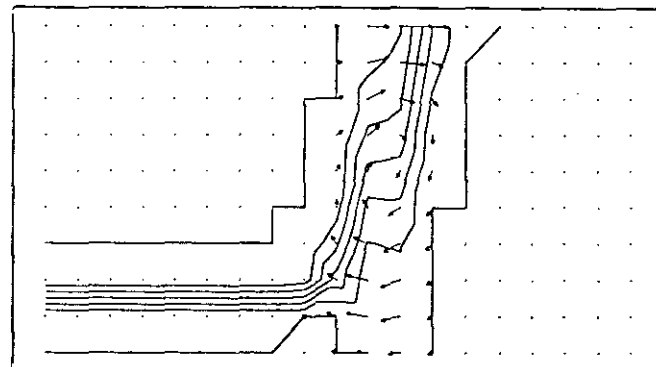
The appearance in the solution of very intense inertial oscillations is a direct consequence of the drastic initial conditions. The adjustment between two fluids has been generally studied in shallow basins and inertial oscillations were then almost always damped after a few inertial periods. In this section we show the significant influence of these oscillations on the recirculation of the buoyant fluid.

The lock between the two water masses was released at $t = 0$ h and we have followed the evolution of the adjustment during 100 h, after which the position of the front is almost invariant. Physically, during the initial stage,



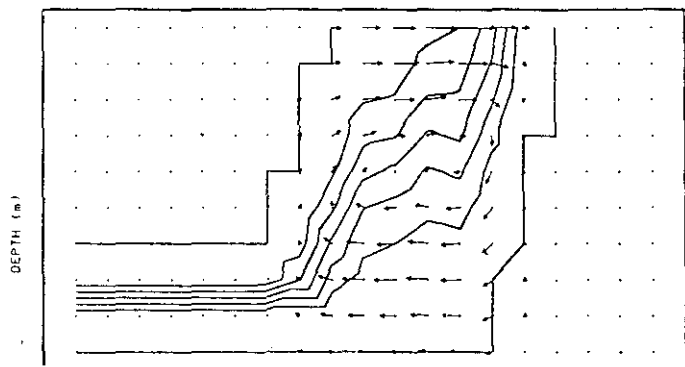
CROSS FRONT DISTANCE (Km)

ADJUSTMENT AFTER 1h (depth=100 m, 1cm=100 cm/s)



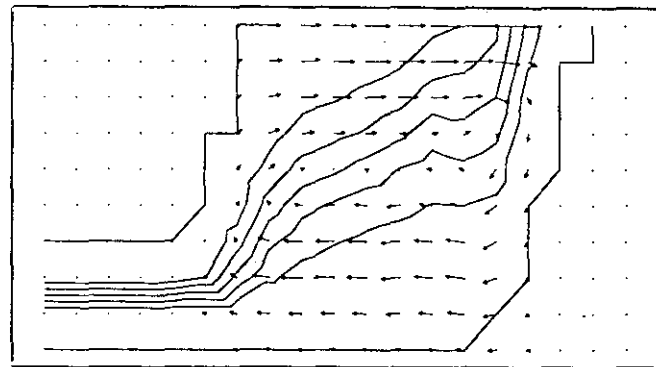
CROSS FRONT DISTANCE (Km)

ADJUSTMENT AFTER 5h (depth=100 m, 1cm=100 cm/s)



CROSS FRONT DISTANCE (Km)

ADJUSTMENT AFTER 10h (depth=100 m, 1cm=100 cm/s)



CROSS FRONT DISTANCE (Km)

ADJUSTMENT AFTER 15h (depth=100 m, 1cm=100 cm/s)

Figure 2.—Cross-frontal velocity and density distribution in the non rotating case, shallow basin during the adjustment process (until 15 h).

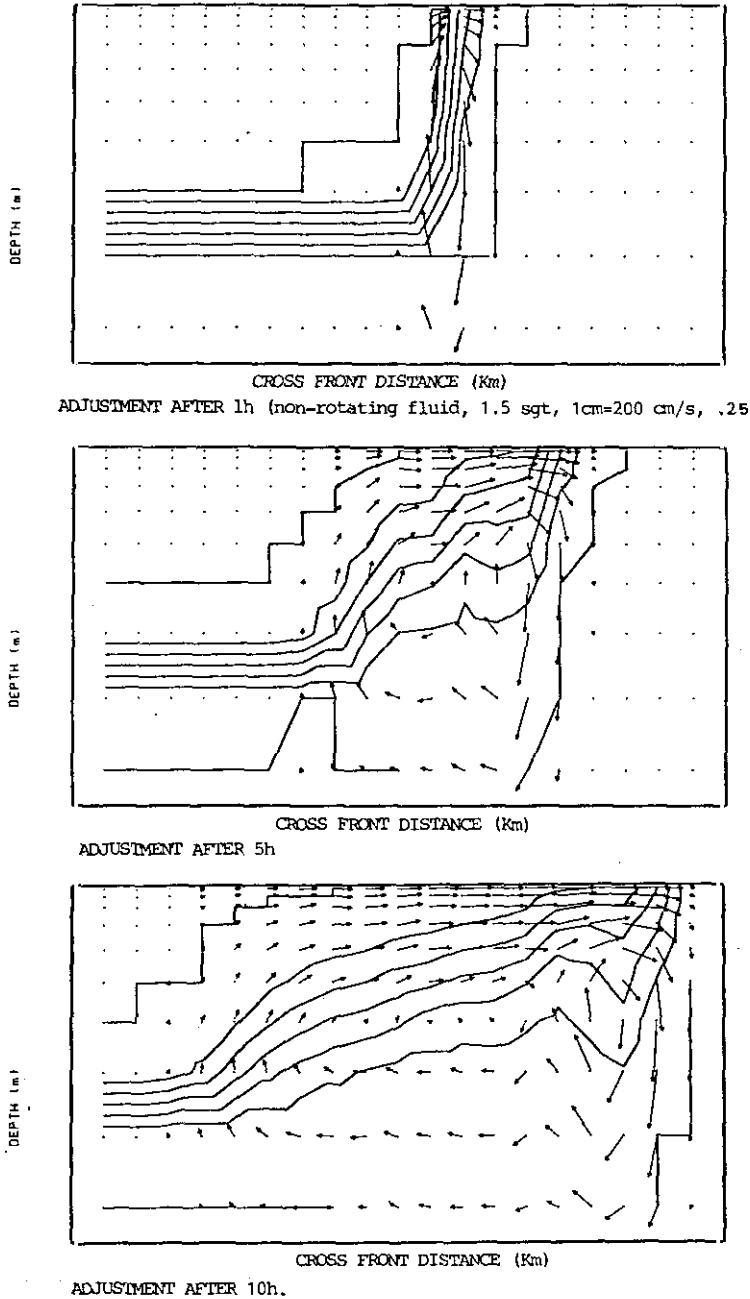


Figure 3.—Cross-frontal circulation and density distribution in the non rotating case, deep basin during the adjustment process (until 10 h).

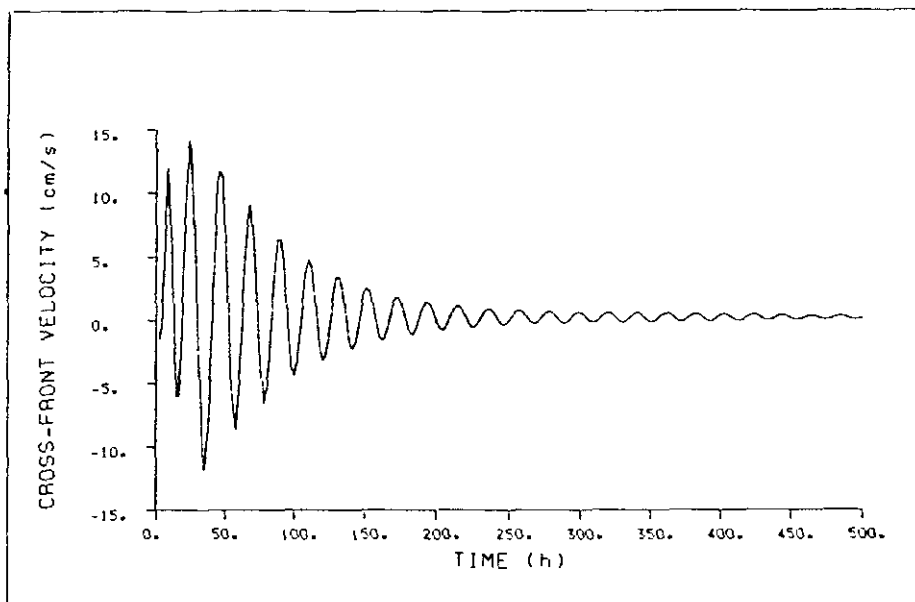


Figure 4.—Horizontal cross-front velocity during the adjustment process (until $t = 500$ h).

the evolution is similar to the non rotating case: a gravity current is formed as a result of the horizontal pressure gradient induced by the buoyancy difference. With rotation however, the forward motion is gradually deflected towards the right, the propagation of the front slows down and a stationary state in quasigeostrophic balance is attained (Kao *et al.*, 1978).

3.2.1. *Shallow basin*

A near steady state is reached after approximately 100 h of simulation. The position of the front is then almost stationary, although inertial oscillations are still present in the velocity field. This is particularly evident in the evolution of the horizontal cross-front velocity, figure 4, which goes through a sequence of oscillations of decaying amplitude. At $t = 100$ h, the oscillations are still very significant, and only at $t = 450$ h, a weak ($.2$ cm/s) but permanent cross-frontal circulation is established.

It is important to note that after 100 h, the steady state reached (it is actually a practical choice for equilibrium) is still very much influenced by the effects of the gravity-inertial waves that induce horizontal velocities at least an order of magnitude higher than the mean. Figure 5 presents the evolution of the adjustment every 10 h and the strong influence of these inertial oscillations on the cross-frontal circulation is clearly demonstrated. At

$t = 100$ h, the alongfront circulation, figure 6, features a surface intensified jet (40 cm/s) with a width of approximately 20 km.

3.2.2. *Deep basin*

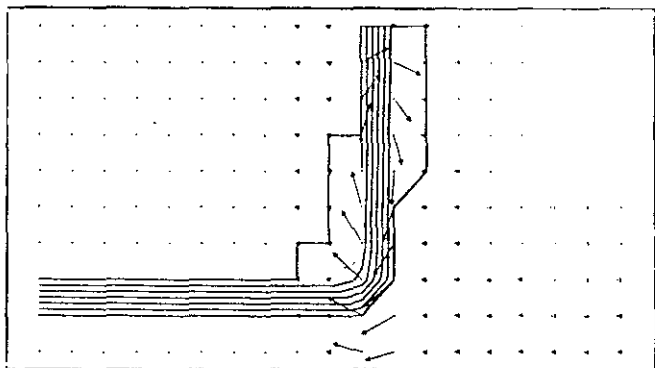
Like in the previous case, the position of the front is almost invariant after 100 h and the cross and along-front circulations are also strongly affected by the inertial oscillations. At $t = 70$ and 90 h (figure 7a) the strong surface convergence induces the subduction of the light fluid. This downward motion is clearly diapycnal in the upper layers but tends to become along-isopycnal below 200 m. The recirculation pattern shows a cell with strong upward motion on the side of the light waters. The patterns observed at $t = 80$ and 100 h, figure 7b, show the same features with reserved signs, the circulation being now opposite to what was found in figure 7a because of the strong inertial oscillations (period around 19h) that dominate the cross-frontal circulation.

The alongfront circulation induced by such an intense density front is formed by an intense baroclinic jet. At $t = 90$ h, the mean along-front velocity was around 70 cm/s and the width approximately 40 km. The baroclinic Rossby Radius of deformation $R_d = ND/f$ is 20 km and therefore the result obtained agrees well with the expected theoretical result. It is important to emphasize the orders of magnitude of the velocities induced. Maximum values for the cross-frontal velocity are of the order of 50 cm/s, while they are around 75 cm/s for the alongfront velocity. Maximum vertical velocities of the order of .3 cm/s are reached at around 200 m.

4. DISCUSSION

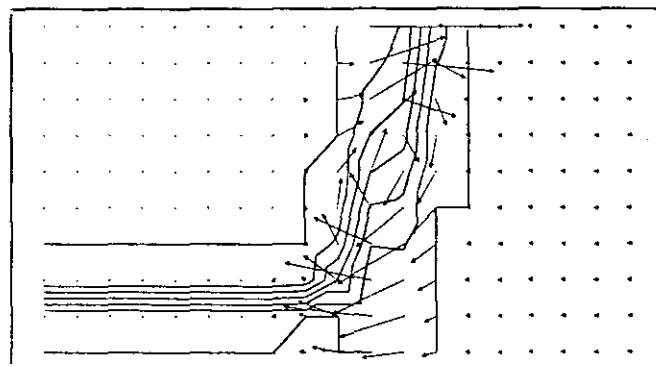
The presence of a recirculating pattern close to the «double cell» circulation proposed by Mooers *et al.* (1976) is without any doubt, figure 7. A similar type of recirculation was found by James (1977, 1984) and Wang (1984) but the induced velocity fields were at least an order of magnitude smaller than the ones obtained here. An essential point is that when this cross-frontal circulation is really significant ($t < 100$ h), it is very strongly modified by the gravity-inertial oscillations (the fluctuating part) generated during the early stage of the adjustment. In other words, the permanent cross-frontal circulation in the sense of James (1984) is strongly dominated by the fluctuating internal-inertial oscillations. The intense vertical motions obtained in this numerical study support the observations of regions of surface convergence or divergence often found in frontal regions (Simpson and James, 1986; Tintoré *et al.*, 1988; Bouchez *et al.*, 1989).

Our results show the adjustment in a shallow basin is clearly different from the adjustment in a deep one. In this last case, the higher depth allows for higher vertical velocities which completely distort the initial density



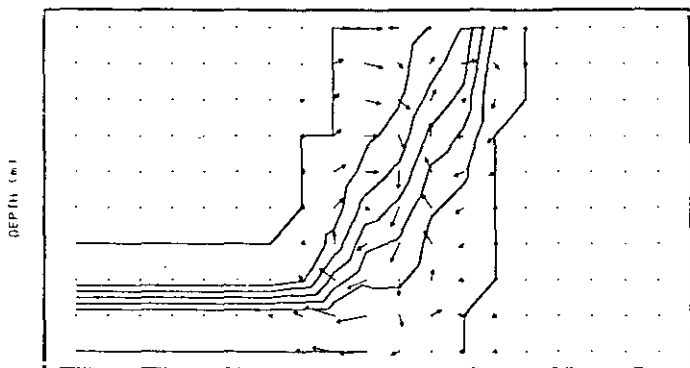
CROSS FRONT DISTANCE (Km)

ADJUSTMENT AFTER 1h (depth=100m, rotation, .25, 1cm=20cm/s)



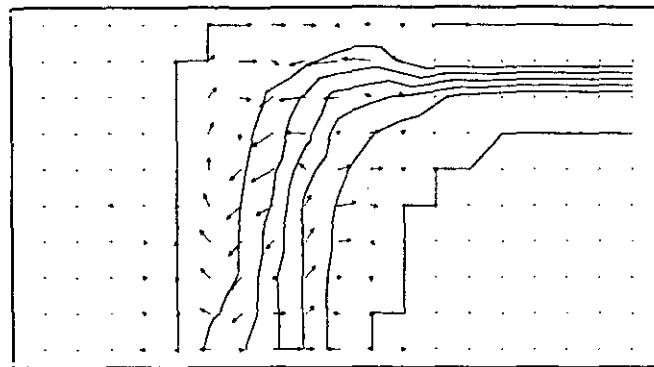
CROSS FRONT DISTANCE (Km)

ADJUSTMENT AFTER 5h



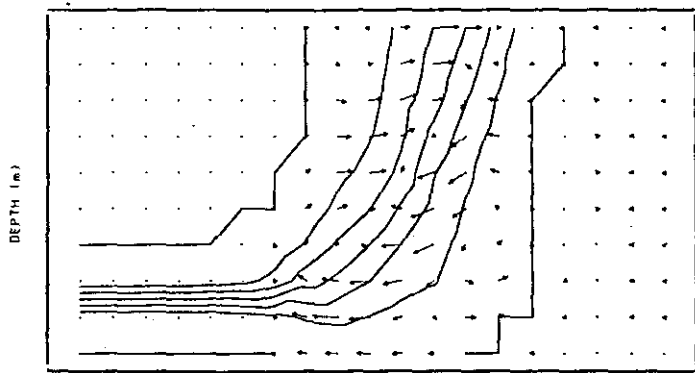
CROSS FRONT DISTANCE (Km)

ADJUSTMENT AFTER 10h



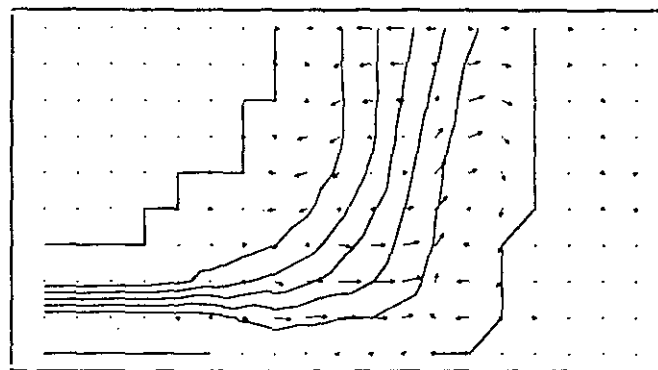
CROSS FRONT DISTANCE (Km)

ADJUSTMENT AFTER 20h



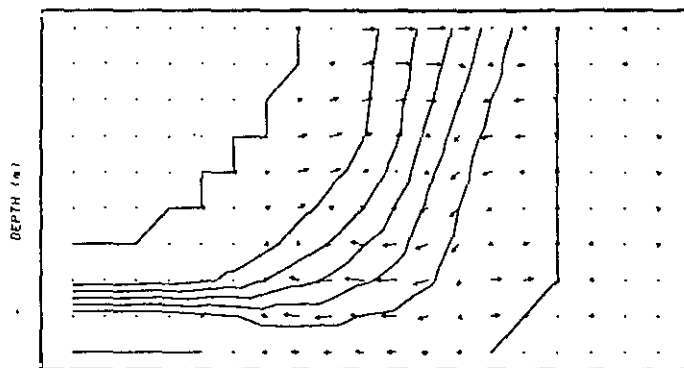
CROSS FRONT DISTANCE (Km)

ADJUSTMENT AFTER 30h



CROSS FRONT DISTANCE (Km)

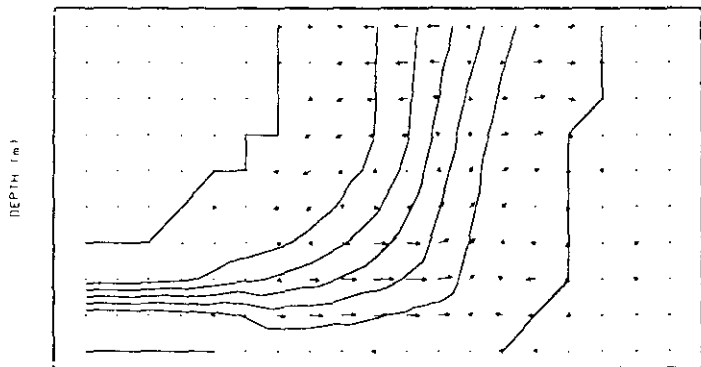
ADJUSTMENT AFTER 40h



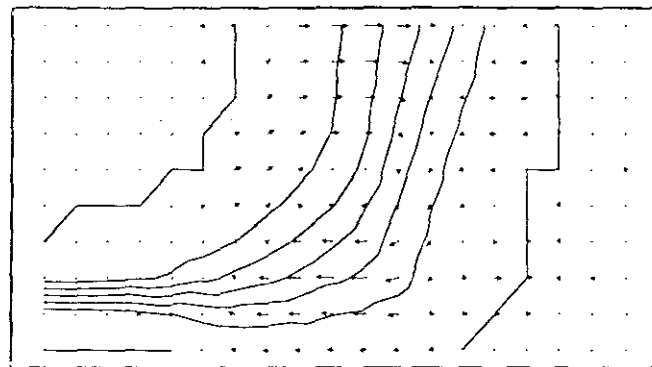
CROSS FRONT DISTANCE (Km)

ADJUSTMENT AFTER 50h

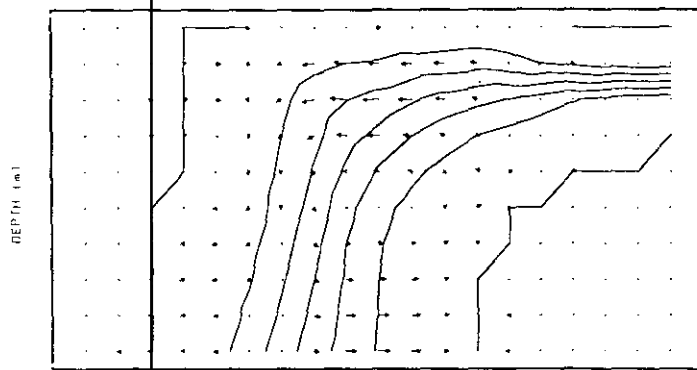
Figure 5. —Cross-frontal velocity and density distribution with rotation and in a shallow basin during the adjustment process (until 110h).



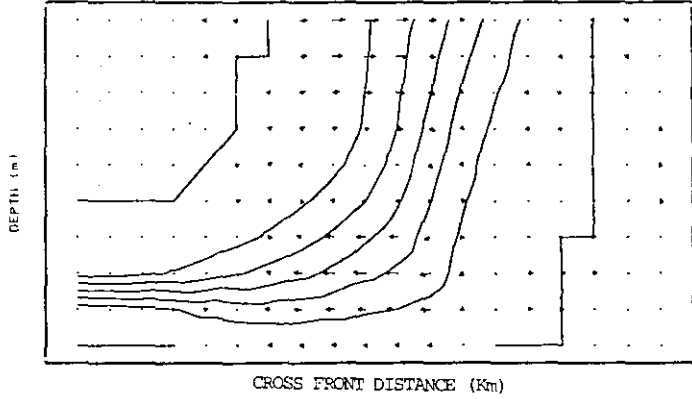
ADJUSTMENT AFTER 60h



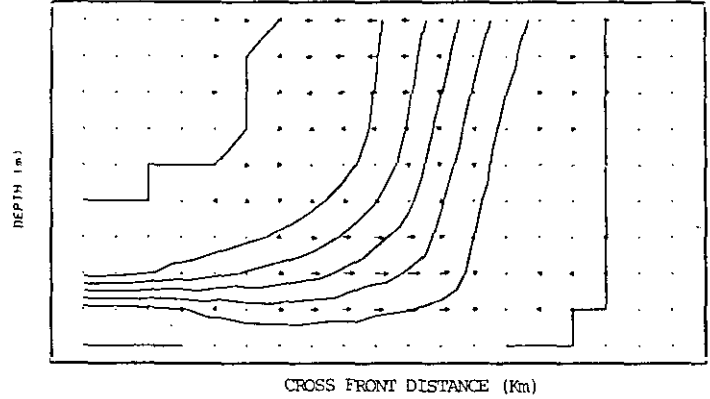
ADJUSTMENT AFTER 70h



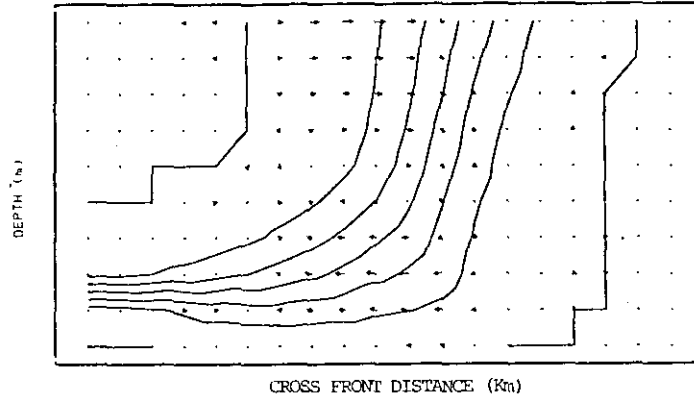
ADJUSTMENT AFTER 80h



ADJUSTMENT AFTER 90h



ADJUSTMENT AFTER 100h



ADJUSTMENT AFTER 110h

Figure 5.—(Continuación.)

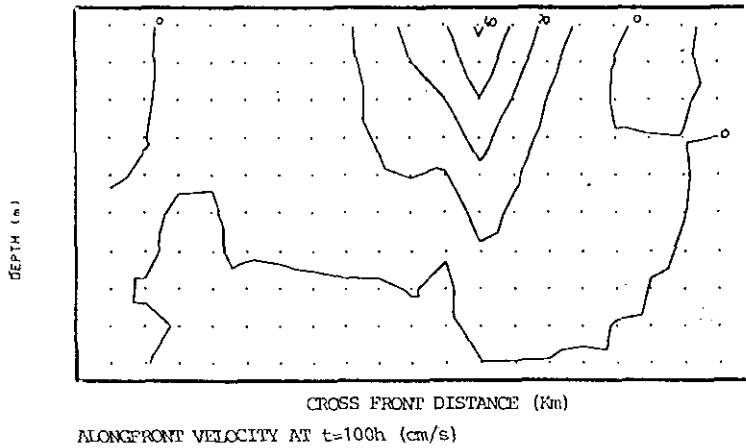


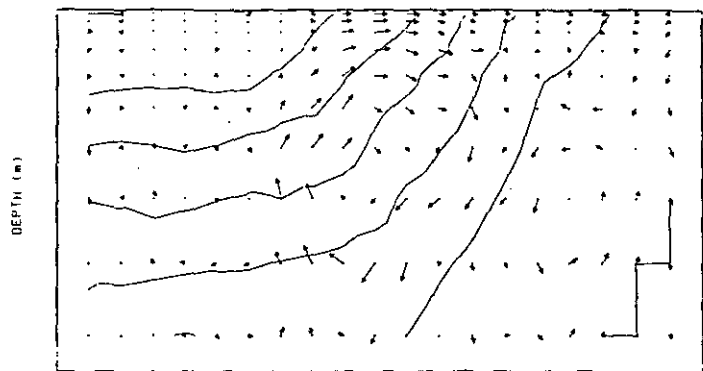
Figure 6.—Alongfront velocity and density distribution with rotation and in a shallow basin at $t = 100h$.

distribution at lower levels. Near the surface, the front is also less sharp as a result of the very intense vertical motions. This suggests that when this type of adjustment occurs in deep basins (like in the Eastern Alboran Sea, where Mediterranean and Atlantic waters converge south of Cape Gata with depths around 1500 m) very strong vertical velocities can be reached as a result of the near-inertial motion. Even in shallow seas (as a result of tidal forcing) the effects of these inertial oscillations has to be considered since the associated vertical motions can have a significant influence on the increased biomass found in tidal fronts.

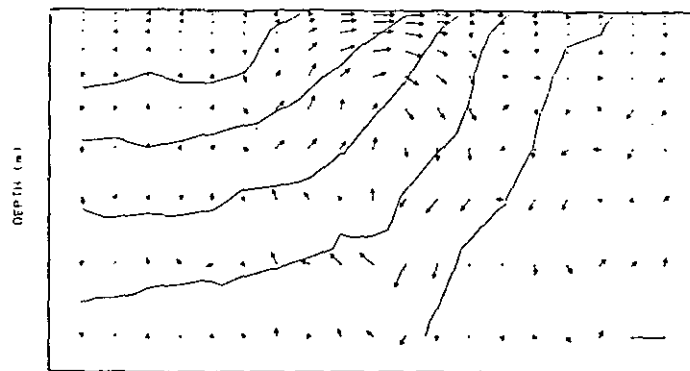
The equilibrium state obtained in this numerical simulation is very close to the situation described by Tintoré *et al.* (1988) for the eastern Alboran Sea Almería-Orán front. For a weaker initial density gradient, the final position of the surface front would have been closer to x_0 (Ou, 1984). Therefore it appears from this numerical study that the formation of this very strong density can be explained in terms of the geostrophic adjustment of the Modified Atlantic Water and the Mediterranean Water that collapse south of Cape Gata. For a weaker initial distribution there are still chances that a sharp front would form because of the contribution of other physical mechanism (not included in this simulation) such as convergence, existence of a horizontal deformation field (Hoskins and Bretherton, 1972).

5. SUMMARY AND CONCLUSIONS

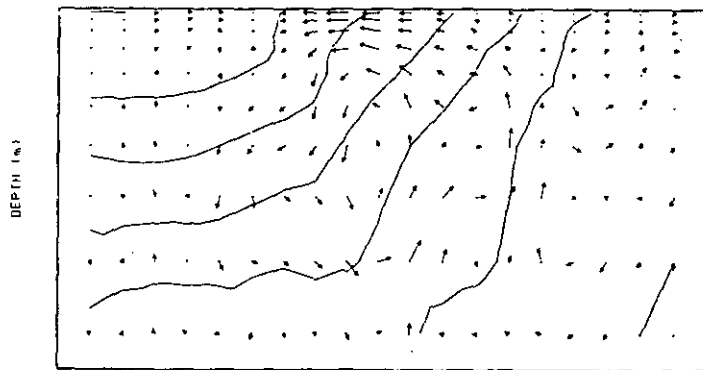
The dynamics of the initial adjustment between two different water masses is representative of the formation of fronts in most shelf regions and of the type of processes occurring in straits. The final steady state dynamics is



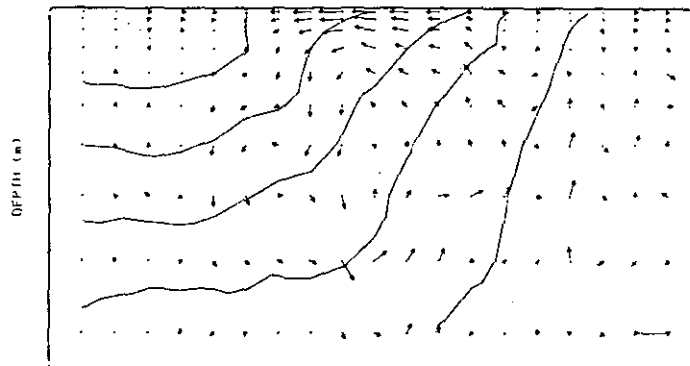
CROSS FRONT DISTANCE (Km)
ADJUSTMENT AFTER 70h



CROSS FRONT DISTANCE (Km)
ADJUSTMENT AFTER 90h



CROSS FRONT DISTANCE (Km)
ADJUSTMENT AFTER 80h



CROSS FRONT DISTANCE (Km)
ADJUSTMENT AFTER 100h

Figure 7.—Cross-frontal velocity and density distribution with rotation in a deep basin at $t=70, 80, 90, 100$ h.

more general and is probably relevant to all kinds of density fronts. The very sharp initial density distribution imposed in this numerical study gives rise to a steady state characterized by a sharp density front with a permanent and very slow ageostrophic circulation. However, we have found that in the early stages of the adjustment ($T = 5/f$), this crossfrontal circulation which depicts a «double cell» pattern, is strongly modified by the internal-inertial waves radiated during the initial adjustment. The velocities obtained were at least one order of magnitude higher than in previous studies, clearly showing the fundamental importance of these inertial oscillations. Their role will have to be considered to fully understand the regions of surface convergence or divergence or the higher biomass often found in frontal regions.

Comparison of these theoretical results with observations in the Alboran Sea indicates that the formation of the permanent density front in the Eastern Alboran Sea can be explained in terms of the geostrophic adjustment of Modified Atlantic Water and Mediterranean Water that collapse south of Cape Gata. The intense vertical motions obtained numerically also support the observations of very close regions of surface convergence and divergence with strong vertical motions and significant biomass increase. A quantitative study of the influence of inertial oscillations on upper ocean circulation and mixing is not yet available. This study is needed for a better understanding of the dynamics of oceanic frontal regions.

Acknowledgements

This work was partially funded by the DGICYT (PB89-0428), the MAST EC program under project EUROMODEL (0043-C) and the CICYT Programa Nacional de Recursos Marinos y Acuicultura (MAR 89-0550) and MAR90-1229E.

REFERENCES

- Armi, L. and D. Farmer (1987): A generalization of the concept of maximal exchange, in a strait. *J. Geophys. Res.* **92**, 679-14.680.
- Benjamin, T. B. (1968): Gravity currents and related phenomena. *J. Fluid Mech.* **31**, 209-48.
- Bouchez, J., F. Ibáñez and L. Prieur (1987): Daily and seasonal variations in the spatial distribution of zooplacton populations in relation to the physical structure in the Ligurian front. *J. Mar. Res.* **45** (1), 133-173.
- Brink, K. H. (1987): Coastal ocean physical processes. *Reviews of Geophysical and Space Physics*, **25**, 2, p. 204-216.
- Csanady, G. T. (1971): On the equilibrium shape of the thermocline in the shore zone. *J. Phys. Oceanogr.* **8**, 47-62.
- Csanady, G. T. (1978): Wind effects on surface to bottom fronts. *J. Geophys. Res.*, **83**, 4633-4640.
- Gill, A. E. (1976): Adjustment under gravity in a rotating channel. *J. Fluid. Mech.* **77**, 603-621.

- Gill, A. E. (1982): *Atmosphere Ocean Dynamics*. Academic Press.
- Hoskins, B. J., Bretherton, F. P. (1972): Atmospheric frontogenesis models: mathematical formulation and solution. *J. Atmos. Sci.* **29**, 11-37.
- James, I. D. (1978): A note on the circulation induced by shallow sea fronts. *Estuarine Coastal Mar. Sci.*, **7**, 197-202.
- James, I. D. (1984): A three dimensional numerical shelf-sea front model with variable eddy viscosity and diffusivity. *Cont. Shelf Res.* **3**, 69-98.
- Kao, T. W., H-P Pao and C. Park (1978): Surface Intrusions, Fronts and Internal Waves: A numerical Study. *J. Geophys. Res.* **83**, 4641-4650.
- Middleton, J. F. (1987): Energetics of linear geostrophic adjustment. *J. Phys. Oceanogr.* **17**, 735-740.
- Mooers, C. N. K., C. A. Collins and R. L. Smith (1978): The dynamic structure of the frontal zone in the coastal upwelling region off Oregon. *J. Phys. Oceanogr.* **6**, 3-21.
- Ou, H. H. (1984): Geostrophic adjustment: A mechanism for frontogenesis. *J. Phys. Oceanogr.* **14**, 994-1000.
- Rossby, C. G. (1937): On the mutual adjustment of pressure and velocity distributions in certain simple current systems: I. *J. Mar. Res.* **1**, 15-28.
- Simmons, T., J., (1980): Circulation model of lakes and inland seas. Can. Bull. Fish. Aquat. Sci: 203-146 p.
- Simpson, J. H. and I. D. James (1986): Coastal and Estuarine fronts». In *Baroclinic Processes on Continental shelves*. C. N. K. Mooers ed., AGU.
- Tintoré, J., P. E. La Violette, I. Blade, A. Cruzado (1988): A study of an intense density front in the Eastern Alboran Sea. *J. Phys. Oceanogr.* **18**, 1384-1397.
- Van Heijst, G. J. F. (1985): A geostrophic adjustment model of a tidal mixing front. *J. Phys. Oceanogr.* **15**, 1182-1190.
- Wang, D. P. (1982): Development of a three-dimensional limited-area (island) shelf circulation model. *J. Phys. Oceanogr.* **12**, 605-617.
- Wang, D. P. (1984): Mutual intrusions of a gravity current and density front formation. *J. Phys. Oceanogr.* **7**, 1191-1199.